Studies of Terbium Bridge: Saturation Phenomenon, Significance of Sensitizer and Mechanisms of Energy Transfer, and Luminescence Quenching

Dawei Wen, Jianxin Shi,* Mingmei Wu,* and Qiang Su

MOE Key Laboratory of Bioinorganic and Synthetic Chemistry/State Key Laboratory of Optoelectronic Materials and Technology, Key Laboratory of Environment and Energy Chemistry of Guangdong Higher Education Institutes, School of Chemistry and Chemical Engineering, Sun Yat-Sen University, No. 135, Xingang Xi Road, Guangzhou 510275, P.R. China

Ⓢ Supporting Information

ABSTRACT: Terbium chain in the form of $S \rightarrow (Tb^{3+})_n \rightarrow A$ ($S = Ce^{3+}$ or Eu^{2+}, $A = Eu^{3+}$), as a promising energy transfer (ET) approach, has been proposed to enhance Eu^{3+} emission for solid-state lighting. However, the viewpoint of ET from S to A via the terbium chain ($Tb^{3+}-Tb^{3+}-Tb^{3+}-...$) is very doubtful. Here, hosts of $Ba_3Ln(PO_4)_3$, $LnPO_4$, $LnBO_3$, and $Na_2Ln_2B_2O_7$ doped with $Ce^{3+} \rightarrow (Tb^{3+})_n \rightarrow Eu^{3+}$ or $(Tb^{3+})_n \rightarrow Eu^{3+}$ are synthesized to prove the universality of $S \rightarrow (Tb^{3+})_n \rightarrow A$ in inorganic hosts and to study the unsolved issues. Saturation distance of $Tb^{3+}-Eu^{3+}$, estimated with the empirical data of different hosts, is proposed to be a criterion for determining whether a spectral chromaticity coordinate keeps constant. A branch model is put forward to replace the chain model to explain the role of $(Tb^{3+})_n$ in ET from Ce^{3+} to Eu^{3+} and the necessity of high content of Tb^{3+}; the term "terbium bridge" is used to replace "terbium chain", and the value of n is determined to be two or three. The intensity quenching of Eu^{3+} emission is attributed to the surface defects ascribed to the smaller particles and larger specific surface area rather than the concentration quenching of Tb^{3+}. Based on the saturation distance and the mechanism of luminescence quenching, the necessary concentration of Tb^{3+} for $(Tb^{3+})_n$ can be estimated as long as the cell parameters are already known and the luminescent efficiency of Eu^{3+} can be further improved by optimizing the synthesis method to decrease the quantity of surface defects.

KEYWORDS: terbium bridge, luminescence, LED, energy transfer, phosphor, sensitization
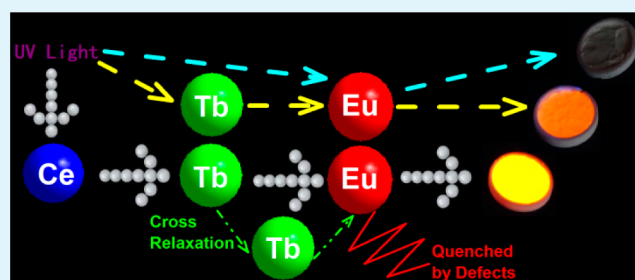
1. INTRODUCTION

Phosphor-converted white-light-emitting diodes (pc-WLEDs) are important candidates for replacing traditional light sources due to their higher efficiency of energy conversion.[1−5] The commercial WLEDs, fabricated by blue-emitting chips coated with the yellow-emitting $Y_3Al_5O_{12}$:Ce^{3+} garnet, have several drawbacks such as a high correlated color temperature (CCT) and a low color-rendering index (CRI). Near-ultraviolet (n-UV) based LEDs with tricolour phosphors, as an alternative to the commercial WLEDs, are attracting attention due to their tunable CRIs and CCTs by adjusting the ratios of tricolour phosphors. Furthermore, the blue component of the commercial WLEDs comes from the blue electroluminescence that bleeds through the phosphor coating, which is strongly dependent on the thickness of the phosphor layer. The ratio of the bleeding blue light and the phosphor-emitting light cannot be precisely controlled in the manufacturing industry, which leads to poor CCTs and CRIs. However, n-UV based LEDs may overcome this defect because human eyes are insensitive to UV-light (350−370 nm), so the CRIs and CCTs are solely controlled by the ratio of tricolour phosphors. This holds potential for color uniformity in the LED packaging industry,

and the pressing issues are the minimization of bleeding UV light and seeking high efficiency tricolor phosphors.

The development of novel red phosphors is key in researching n-UV based WLEDs due to the poor efficiency of traditional red phosphors such as Y_2O_3:Eu^{3+} and Y_2O_2S:Eu^{3+} under 350−400 nm excitation.[6−9] Some efficient red phosphors such as $Lu_2CaMg_2(Si,Ge)_3O_{12}$:$Ce^{3+}$ and $Ca_4(PO_4)_2O$:Eu^{2+} encounter the shortcoming of absorption in the green region.[10,11] Sensitization may enhance the UV excitation with no obvious absorption in the blue and green region. Some trivalent rare-earth ions with an $f-f$ forbidden transition can be effectively sensitized by Ce^{3+} or Eu^{2+} ions with the $f-d$ allowed transition. However, the narrow line red or orange light-emitting ions such as Eu^{3+} and Sm^{3+} cannot be directly sensitized by Ce^{3+} or Eu^{2+} ions ascribed to the existence of metal−metal charge transfer (MMCT), which quenches the luminescence of the sensitizer.[12−14]

Recently, a terbium chain has been put forward as an intermediate to alleviate the MMCT effect in the host of YBO_3 by A. A. Setlur.[15] A novel model of S → $(Tb^{3+})_n$ → A was formed to explain the enhancement of the narrow line red luminescent intensity of n-UV pumped phosphors. Here, "S" represents the sensitizers with the allowed transition and "A" represents the activators with the forbidden transition. Jia et. al reported the enhancement of luminescent intensity of Sm^{3+} ions by realizing Eu^{2+} → $(Tb^{3+})_n$ → Sm^{3+} in the host of $Sr_3Ln(PO_4)_3$.[16] Eu^{2+} → $(Tb^{3+})_n$ → Eu^{3+} in the host of $Ba_2Ln(BO_3)_2Cl$ was a meaningful example for the application of the terbium chain, and the tunable emission from green to orange was realized by increasing the content of Tb^{3+}, though the mixed valence phenomenon of europium ions is uncontrollable.[17] $(Tb^{3+})_n$ → Mn^{2+} in $Sr_3Tb(PO_4)_3$ was a special form because it is a simplified one without a sensitizer.[18] The simplified form, $(Tb^{3+})_n$ → A, is an issue deserving research because the MMCT effect is entirely alleviated in such a form that the luminescent intensity might have a potential increase. In hosts of $Sr_3Ln(PO_4)_3$ and $Ba_2Ln(BO_3)_2Cl$ as mentioned above, a high content of Tb^{3+} (90%) is necessary to achieve a sufficient energy transfer (ET) and a stable spectral chromaticity coordinate. In $Na_2Y_2B_2O_7$, we realized a constant chromaticity coordinate by the complete ET from Tb^{3+} to Eu^{3+} in Ce^{3+} → $(Tb^{3+})_n$ → Eu^{3+} with a relatively low content of Tb^{3+} (45%−60%) and put forward a saturation distance between terbium ions to explain the low concentration phenomenon.[19] Based on our theory, Ce^{3+} → $(Tb^{3+})_n$ → Eu^{3+} with a low concentration of Tb^{3+} in other hosts is expected to be realized. The research on the terbium chain was also extended to oxynitride.[20] The ET from Tb^{3+} to Eu^{3+} is insufficient, so the green emission of Tb^{3+} is obviously observed with a lower concentration of Tb^{3+} and an evident quenching of Eu^{3+} with a higher concentration of Tb^{3+}.[20] A similar quenching phenomenon of Eu^{3+} with a high content of Tb^{3+} was also observed in our previous work.[19] However, the explanation is different, with the mineral constitution affecting luminescent properties versus the concentration quenching of Tb^{3+}.[20]

S → $(Tb^{3+})_n$ → A is a promising method to enhance the red emission of $f−f$ transition ions such as Eu^{3+}, but the previous research efforts were relatively independent and the universal rule of obtaining a constant chromaticity coordinate is not obvious. The saturation phenomenon of Tb^{3+} has never been investigated systematically, and the reproducibility of this phenomenon in other hosts is unknown. In S → $(Tb^{3+})_n$ → A, the contents of S and A are usually less than 1%, while the content of Tb^{3+} is up to 30%−99%.[15,16,18−21] The terbium chain ($Tb^{3+}−Tb^{3+}−Tb^{3+}−...$) is usually used to explain the ET from S to A. The point of view is very doubtful due to the lack of direct evidence for the continuous ET among Tb^{3+} ions. The reason why a relatively high Tb^{3+} content (≥30%) is necessary for the formation of the terbium chain is still a mystery. Furthermore, the efficiency of sensitizer-free $(Tb^{3+})_n$ → Eu^{3+} to enhance the emission of Eu^{3+} is never studied. Finally, the mechanism for luminescence quenching of Eu^{3+} with a higher Tb^{3+} content is also unclear.

In this work, we focus on the Ce^{3+} → $(Tb^{3+})_n$ → Eu^{3+} system rather than the Eu^{2+} → $(Tb^{3+})_n$ → Eu^{3+} one because the ratio and coexistence of europium ions are mysteries in most hosts. Ce^{3+} → $(Tb^{3+})_n$ → Eu^{3+} or $(Tb^{3+})_n$ → Eu^{3+} is introduced into hosts of $Ba_3Ln(PO_4)_3$, $LnPO_4$, $Na_2Ln_2B_2O_7$, and $LnBO_3$ (Ln = Gd, Lu or Y), among which the space groups and the distances of $Ln^{3+}−Ln^{3+}$ are different, to prove the universality of Ce^{3+} →

$(Tb^{3+})_n$ → Eu^{3+} in inorganic hosts and to study some unsolved issues, such as demonstration of an empirical saturation distance for Ce^{3+} → $(Tb^{3+})_n$ → Eu^{3+}, establishment of a model to explain the potential value of sensitizer-free $(Tb^{3+})_n$ → Eu^{3+}, the significance of the sensitizer, and the mechanism for luminescence quenching of Eu^{3+} with a higher content of Tb^{3+}. Moreover, a branch model is proposed to explain the ET from Ce^{3+} to Eu^{3+} and the necessity of high Tb^{3+} content for Ce^{3+} → $(Tb^{3+})_n$ → Eu^{3+}, and the term "terbium bridge" is used to replace "terbium chain". The results indicate the existence of an empirical saturation distance of $Tb^{3+}−Eu^{3+}$ for the terbium bridge, the necessity of a sensitizer, and the significance of the defect effect on the luminescence quenching of Eu^{3+}. By introducing a promising form of the terbium bridge and decreasing the quantity of surface defects, we can reduce the luminescent quenching effect.

2. EXPERIMENTAL METHODS

2.1. Sample Preparation. The raw materials are $BaCO_3$ (A.R.), $(NH_4)_2HPO_4$ (A.R.), $NaHCO_3$ (A.R.), H_3BO_3 (A.R.), CeO_2 (99.99%), Eu_2O_3 (99.99%), Gd_2O_3 (99.99%),Tb_4O_7 (99.99%), and Lu_2O_3 (99.99%).

Stoichiometric amounts of raw materials were mixed, ground, and sintered under various conditions, respectively. The conditions are presented in Table S1.

2.2. Sample Characterization. Powder X-ray diffraction (XRD) data were collected on a Rigaku D-max 2000 X-ray diffractometer with Cu K_α radiation (λ = 1.5405 Å) to characterize the purity of the phosphor samples and calculate the cell parameters. Photoluminescence (PL) and PL excitation (PLE) spectra were obtained on FPS 920 Time Resolved and Steady State Fluorescence Spectrometers (Edinburgh Instruments) with a 450 W xenon light source. Fluorescence decay time curves were measured using a 150 W nF900 ns flash-light source on the same instrument.
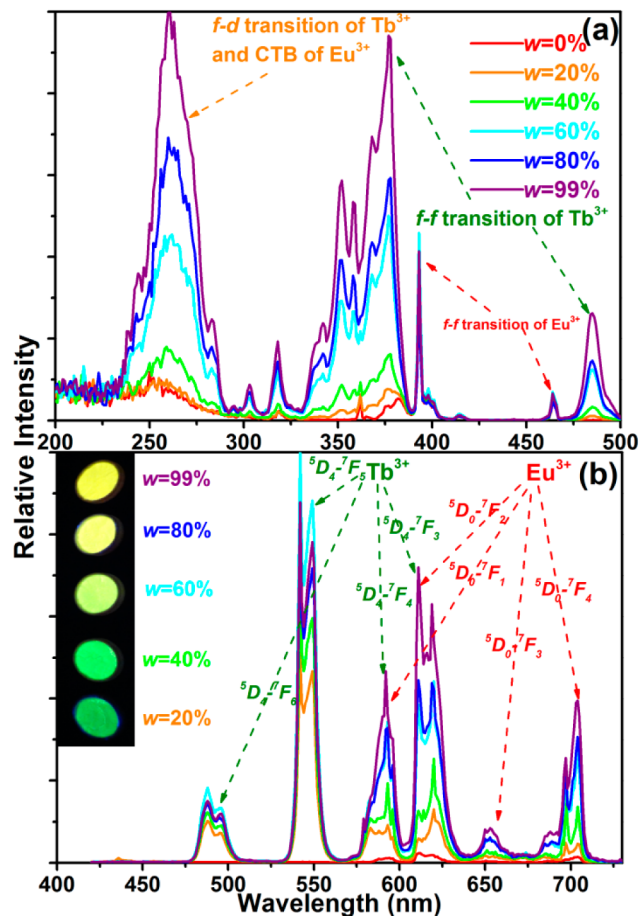
3. RESULTS AND DISCUSSIONS

3.1. Phase and Cell Parameters. In order to compare with previous reports and obtain some general information on S → $(Tb^{3+})_n$ → A, typical hosts of $Ba_3Ln(PO_4)_3$, $LnPO_4$, $LnBO_3$, and $Na_2Ln_2B_2O_7$ were chosen. Among those hosts, the distances of $Ln^{3+}−Ln^{3+}$ are different so that the universality of the distance effect in the terbium bridge can be proved. Rietveld refinements were performed to verify the purity of the phases and calculate the cell parameters, especially the cell volume (V) so as to lay a foundation to analyze the saturation phenomenon and the distances between Tb^{3+} ions. The structure parameters of $Ba_3La(PO_4)_3$,[22] $TbPO_4$,[23] $GdBO_3$,[24] and $Na_2Gd_2B_2O_7$[25] were used as initial parameters for $Ba_3Ln(PO_4)_3$, $LnPO_4$, $LnBO_3$, and $Na_2Ln_2B_2O_7$ in the Rietveld analysis, respectively. The representative results are shown in Figure 1, Tables S2 and S3. Here, $Ba_3Ln(PO_4)_3$ and $LnPO_4$ are representatives of phosphates. Rare earth ions occupy a single site ($4a$) in $LnPO_4$ which belongs to $I41/amd$ (no. 141) tetragonal framework. In $Ba_3Ln(PO_4)_3$, Ba^{2+} and rare earth ions are disordered in a single crystallographic site ($16c$) in the cubic space group $I43d$ (no. 220), so the average distances of the rare earth ions are longer than those in $LnPO_4$. A similar comparison can be found in borates, $LnBO_3$ ($P63/mmc$ (no. 194) - hexagonal), and $Na_2Ln_2B_2O_7$ ($P121/C1$ (no. 14) - monoclinic). $GdBO_3$ and $LuBO_3$ are isostructures, in which rare earth ions occupy the $2a$ site. In $Na_2Ln_2B_2O_7$, two different sites ($4e$) are occupied by rare earth ions.[26] Doping a high concentration of Tb^{3+} ions will not produce a new phase in those polycrystals due to the isostructure properties.
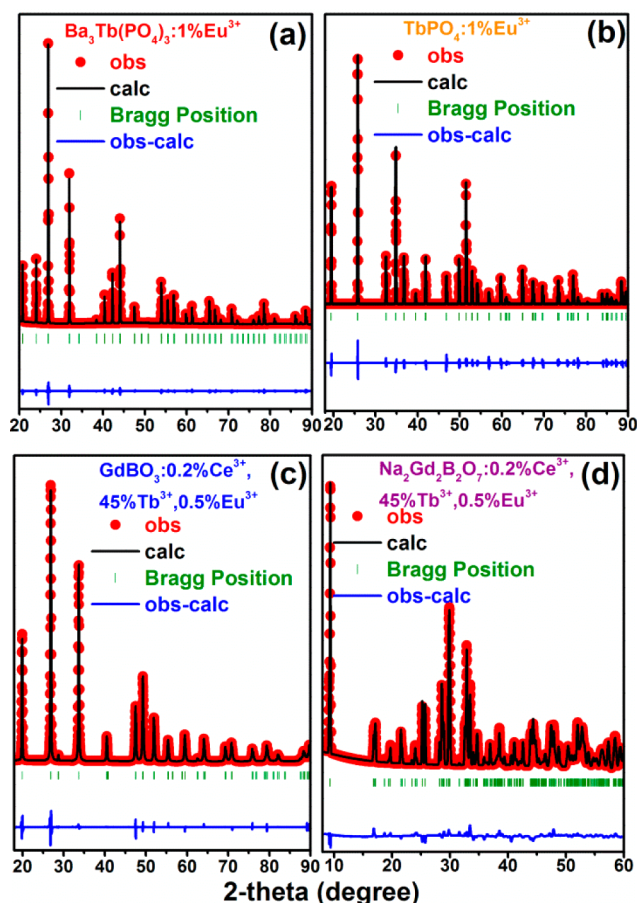
Figure 1. Refinement results and crystal structures of $Ba_3Tb(PO_4)_3$:1%Eu^{3+} (a), $TbPO_4$:1%Eu^{3+} (b), $GdBO_3$:0.2%Ce^{3+},45%Tb^{3+},0.5%Eu^{3+} (c), and $Na_2Gd_2B_2O_7$:0.2%Ce^{3+},45%Tb^{3+},0.5%Eu^{3+} (d).

Figure 2. Photoluminescence excitation (λ_{Em} = 611 nm) (a), Photoluminescence spectra (λ_{Ex} = 377 nm) (b), and digital photos in 365 nm UV box (inset in (b)) of $Ba_3Lu(PO_4)_3$:$w$$Tb^{3+}$,1%$Eu^{3+}$.

3.2. Saturation Phenomenon and Saturation Distance of Terbium Bridge in Phosphates. A sensitizer-free terbium bridge in the form of $(Tb^{3+})_n$-Eu^{3+} is introduced into $Ba_3Lu(PO_4)_3$ and YPO_4 due to the poor n-UV excitation of Ce^{3+} in these hosts.[27,28] The enhancing effect of the sensitizer-free terbium bridge will be discussed in the following sections. The PLE spectra of $Ba_3Lu(PO_4)_3$:$w$$Tb^{3+}$,1%$Eu^{3+}$ monitored at 611 nm are depicted in Figure 2a. The f–d and f–f transitions of Tb^{3+} are becoming stronger gradually with increasing doping content of Tb^{3+} ions, while the f–f transitions intensity of Eu^{3+} ($^7F_0 \rightarrow {}^5D_3$ peaked at 393 nm and $^7F_0 \rightarrow {}^5D_1$ peaked at 464 nm) almost remains constant. The corresponding emission spectra excited at 377 nm are presented in Figure 2b. The emission of Tb^{3+} increases and then decreases while the intensity of Eu^{3+} increases continuously with increasing the content of Tb^{3+}. The results indicate that there is ET from Tb^{3+} to Eu^{3+} in the host of $Ba_3Lu(PO_4)_3$. However, the green emission of Tb^{3+} is still obvious with the high concentration of Tb^{3+} (99%) and the chromaticity coordinate is still shifting. This is a special phenomenon in contrast to the previous reports in which the green emission is almost completely undetected and the chromaticity coordinate is constant in a relatively low content of Tb^{3+} (45%−60%) in YBO_3[15] or $Na_2Y_2B_2O_7$.[15,19] The ET is incomplete even though the content of Tb^{3+} is over 90% in $Ba_3Lu(PO_4)_3$, which leads to a yellow emission combined with the green of Tb^{3+} and red of Eu^{3+}.

This indicates that the concentration of Tb^{3+} might be the inferior requirement to form terbium bridge.

It is significant to analyze the forming condition of a terbium bridge because it forms in various concentrations for different hosts.[15,17,19,20] The distances of Tb^{3+} ions in different concentrations are focused and compared due to the ruleless forming concentration and the deep connection of ET and ions distance. The decay curves of Tb^{3+} in $Ba_3Lu(PO_4)_3$:$w$$Tb^{3+}$,1%$Eu^{3+}$ and CIE chromaticity diagram are depicted in Figure 3, and the detailed information on the chromaticity coordinate, distance between Tb^{3+}–Eu^{3+} ions (R), and average decay time (τ) are presented in Table 1. The values of R and τ are calculated by eqs 1[29] and 2[30] respectively.
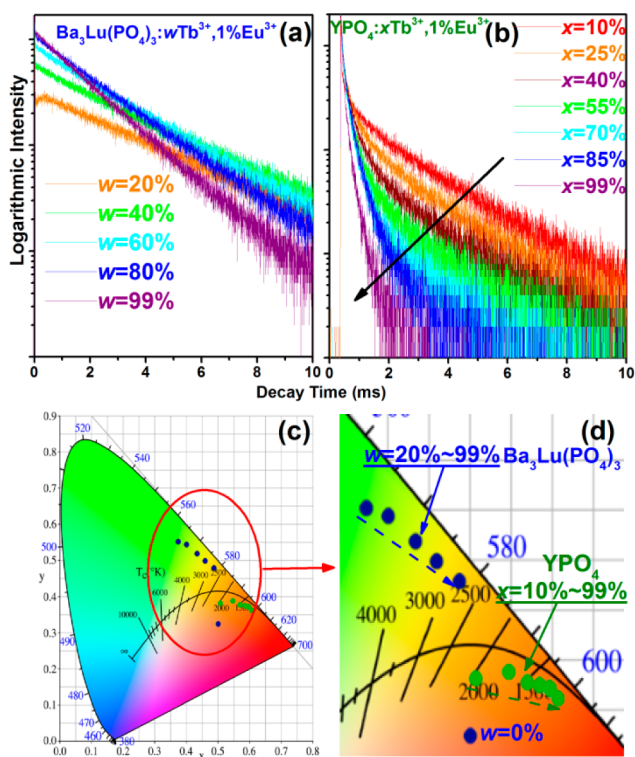
$$R = 2\left[\frac{3V}{4\pi xN}\right]^{1/3} \tag{1}$$

$$\tau = \frac{\int_0^\infty I(t)t \ dt}{\int_0^\infty I(t) \ dt} \tag{2}$$

where V is the volume of the unit cell, N is the number of certain ions in the unit cell, x is the total concentration of Tb^{3+} and Eu^{3+} ions in the host, and $I(t)$ is the luminescent intensity at time t.

The shifting from green to red of the chromaticity coordinate and the decreasing average decay time of Tb^{3+} with increasing content of Tb^{3+} ions in $Ba_3Lu(PO_4)_3$ indicate the strengthening

Figure 3. Decay curves for the emission at 542 nm of Tb^{3+} ions in $Ba_3Lu(PO_4)_3$:wTb^{3+},1%Eu^{3+} (λ_{Ex} = 377 nm) (a), YPO_4:xTb^+,1%Eu^{3+} (λ_{Ex} = 378 nm) (b), and the corresponding CIE chromaticity diagrams (c) and (d).
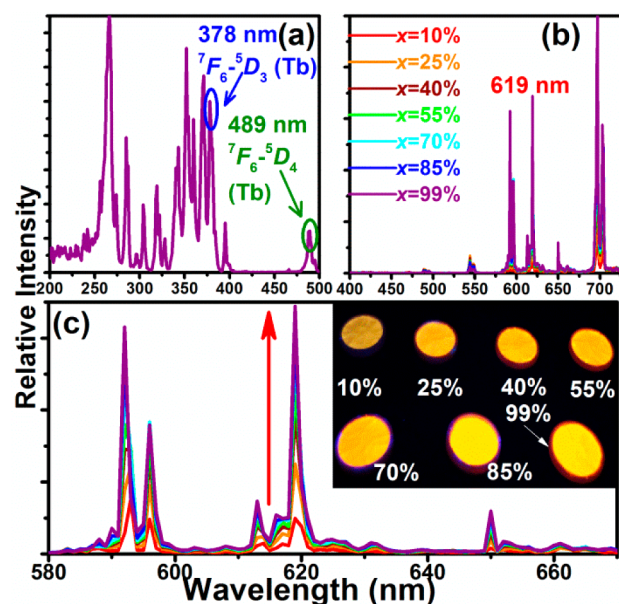
Table 1. Chromaticity Coordinate, R (Tb^{3+}-Eu^{3+}), and τ of Tb^{3+} Emission with Various Tb^{3+} Concentrations in $Ba_3Lu(PO_4)_3$:wTb^{3+},1%Eu^{3+} and YPO_4:xTb^{3+},1%Eu^{3+}, Respectively

$Ba_3Lu(PO_4)_3$			
Tb^{3+}%	chromaticity coordinate	R (Å)	τ (ms)
0%	(0.50, 0.33)	–	–
20%	(0.37, 0.55)	13.76	2.99
40%	(0.40, 0.54)	11.01	2.84
60%	(0.44, 0.52)	9.65	2.50
80%	(0.46, 0.50)	8.78	2.17
99%	(0.49, 0.48)	8.18	1.79
YPO_4			
Tb^{3+}%	chromaticity coordinate	R (Å)	τ (ms)
10%	(0.51, 0.38)	10.75	2.24
25%	(0.55, 0.39)	8.08	1.70
40%	(0.57, 0.38)	6.94	1.35
55%	(0.58, 0.37)	6.27	1.09
70%	(0.59, 0.37)	5.79	0.87
85%	(0.59, 0.37)	5.44	0.72
99%	(0.60, 0.37)	5.18	0.57

ET from Tb^{3+} to Eu^{3+} ions. However, the chromaticity coordinate shifting is incessant and it fails to shift into the red region even though the content of Tb^{3+} is up to 99%, being in contrast to the low content of Tb^{3+} ions (45%−60%) with a constant chromaticity coordinate and red emission in YBO_3.[15,19] Obviously, the insufficient ET of $Tb^{3+} \rightarrow Eu^{3+}$ is responsible for the conspicuous green emission of Tb^{3+} and the incessant chromaticity coordinate shifting in $Ba_3Lu(PO_4)_3$. And

the distance of Tb^{3+}−Eu^{3+} should be responsible for the insufficient ET. Therefore, we put forward a hypothesis that a terbium bridge is completely formed, corresponding to a constant chromaticity coordinate and indicating an unchanged shape of PL spectra, when the average distance of Tb^{3+}−Eu^{3+} ions is less than the empirical saturation distance. Here, the value of R(Tb^{3+}−Eu^{3+}) in $Ba_3Tb(PO_4)_3$:1%Eu^{3+} is calculated to be 8.18 Å, which is too large for Tb^{3+} to sufficiently transfer its energy to Eu^{3+} and corresponding to the unsaturation phenomena of yellow emission and incessant shifting of the chromaticity coordinate. Similar unsaturation phenomena were observed in $Ba_2Tb(BO_3)_2Cl$:Eu^{2+},Eu^{3+},[17,21] in which the distance of Ln^{3+}−Ln^{3+} is always over 7.2 Å, being still too long for ET of $Tb^{3+} \rightarrow Eu^{3+}$.

In YPO_4, the saturation phenomenon is expected to be observed due to the shorter distances between rare earth ions. As presented in Figures 3b−d and 4, a gradual changing of

Figure 4. Photoluminescence excitation spectrum of $TbPO_4$:1%Eu^{3+} (a), Photoluminescence spectra of YPO_4:xTb^{3+},1%Eu^{3+} with excitation of 378 nm (b), amplifying version of PL spectra (c) and photos of the corresponding samples in 365 nm UV box (inset in (c)).

spectra, decreasing decay time, and shifting chromaticity coordinate are observed, indicating the successful formation of a terbium bridge in YPO_4. The changing trend of the chromaticity coordinate in YPO_4:xTb^{3+},1%Eu^{3+} with increasing Tb^{3+} content is shown in Table 1. The shifting of the chromaticity coordinate becomes unclear when the total concentration of the Tb^{3+} and Eu^{3+} ions is over 41%, which shows that the saturation phenomenon is observed when the distance of Tb^{3+}−Eu^{3+} is shorter than 6.94 Å.

The obtained value of R(Tb^{3+}−Eu^{3+}), 6.94 Å, may serve as an empirical distance for the terbium bridge in other hosts as long as the cell parameters are known. Therefore, the terbium bridge in the form of $Ce^{3+} \rightarrow (Tb^{3+})_n \rightarrow Eu^{3+}$ is introduced into borate compounds, $GdBO_3$ and $Na_2Gd_2B_2O_7$, to confirm the universality of the value.
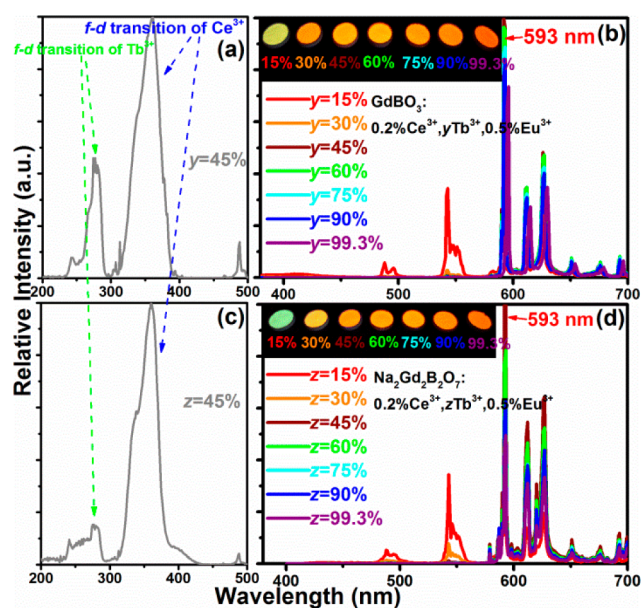
3.3. Application of the Empirical Saturation Distance in Borates Doped with Terbium Bridge. We obtained the empirical saturation distance of Tb^{3+}−Eu^{3+} (6.94 Å) for $LnPO_4$ in the above section. Equation 1 is rewritten to confirm the

universal applicability of the empirical saturation distance in estimating the appropriate saturation content of Tb^{3+} in other hosts doped with a terbium bridge:
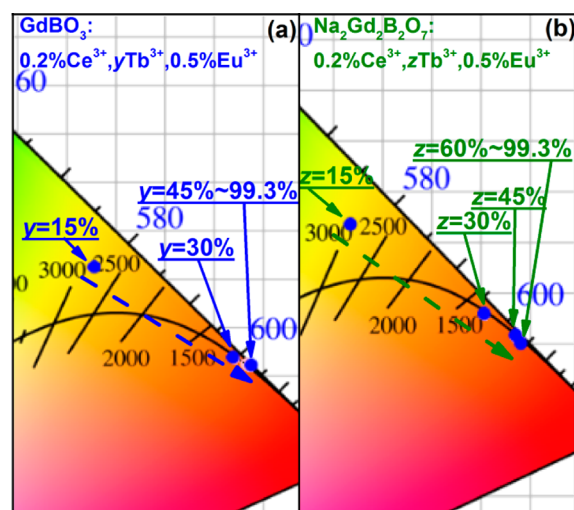
$$x = \frac{6V}{R^3 \pi N} \tag{3}$$

where $N = 2$ and 8 for GdBO$_3$ and Na$_2$Gd$_2$B$_2$O$_7$, respectively, R = 6.94 Å, and V is the volume of the unit cell, which is calculated through refinement and shown in Table S2. The doping of Tb^{3+} has little influence on the volume of the two hosts, 113.9−113.1 Å^3 for LnBO$_3$ and 622.8−620.7 Å^3 for Na$_2$Ln$_2$B$_2$O$_7$. The values of saturation concentration x, the sum of Tb^{3+} and Eu^{3+}, are estimated by putting the values into eq 3, and the results are 32.31%−32.54% and 44.33%−44.48% for LnBO$_3$ and Na$_2$Ln$_2$B$_2$O$_7$, respectively.

Experiments introducing a terbium bridge into LnBO$_3$ and Na$_2$Ln$_2$B$_2$O$_7$ hosts were done to confirm the estimation. The doping contents of Ce^{3+} and Eu^{3+} are fixed to 0.2% and 0.5% respectively to alleviate the MMCT effect in borates. As presented in Figure 5a and c, the broad bands in the n-UV

Figure 5. Photoluminescence excitation ($y = 45\%$, λ_{Em} = 593 nm) (a), photoluminescence spectra (λ_{Ex} = 361 nm) (b) of GdBO$_3$:0.2% Ce^{3+},yTb^{3+},0.5%Eu^{3+}, PLE ($z = 45\%$, λ_{Em} = 593 nm) (c), photoluminescence spectra (λ_{Ex} = 360 nm) (d) of Na$_2$Gd$_2$B$_2$O$_7$:0.2%Ce^{3+},zTb^{3+},0.5%Eu^{3+}, and photos of the corresponding samples in 365 nm UV box (insets in (b) and (d)).

range in the PLE spectra of GdBO$_3$:0.2%Ce^{3+},45%Tb^{3+},0.5% Eu^{3+} and Na$_2$Gd$_2$B$_2$O$_7$:0.2%Ce^{3+},45%Tb^{3+},0.5%Eu^{3+} indicate the sensitization effect of Ce^{3+} ions. The PL spectra of GdBO$_3$:0.2%Ce^{3+},yTb^{3+},0.5%Eu^{3+} and Na$_2$Gd$_2$B$_2$O$_7$:0.2% Ce^{3+},zTb^{3+},0.5%Eu^{3+} are shown in Figure 5b and d, illustrating that, with increasing content of Tb^{3+}, the green emission of Tb^{3+} decreases, while the red emission of Eu^{3+} increases first and then decreases. The results demonstrate the ET from Tb^{3+} to Eu^{3+} and the formation of a terbium bridge, Ce^{3+} → (Tb^{3+})$_n$ → Eu^{3+}, in the two hosts. The relative intensity of the emission with different concentrations of Tb^{3+} will be discussed in the next section. Here, the chromaticity coordinate and R(Tb^{3+}− Eu^{3+}) of the two phosphors are depicted in Figure 6 and Table 2. It can be observed that the chromaticity coordinate shifts to

Figure 6. CIE chromaticity diagrams of GdBO$_3$:0.2%Ce^{3+},yTb^{3+},0.5% Eu^{3+} (a) and Na$_2$Gd$_2$B$_2$O$_7$:0.2%Ce^{3+},zTb^{3+},0.5%Eu^{3+} (b).

Table 2. Chromaticity Coordinate and R (Tb^{3+}−Eu^{3+}) with Various Tb^{3+} Concentrations in GdBO$_3$:0.2% Ce^{3+},yTb^{3+},0.5%Eu^{3+} and Na$_2$Gd$_2$B$_2$O$_7$:0.2%Ce^{3+},zTb^{3+},0.5% Eu^{3+}, respectively

GdBO$_3$		
Tb^{3+}%	chromaticity coordinate	R (Å)
15%	(0.48, 0.46)	8.89
30%	(0.62, 0.37)	7.09
45%	(0.63, 0.36)	6.20
60%	(0.64, 0.36)	5.64
75%	(0.64, 0.36)	5.23
90%	(0.64, 0.36)	4.92
99.3%	(0.64, 0.36)	4.77
Na$_2$Gd$_2$B$_2$O$_7$		
Tb^{3+}%	chromaticity coordinate	R (Å)
15%	(0.47, 0.47)	9.86
30%	(0.60, 0.38)	7.87
45%	(0.64, 0.36)	6.89
60%	(0.64, 0.36)	6.26
75%	(0.64, 0.35)	5.82
90%	(0.64, 0.35)	5.47
99.3%	(0.64, 0.35)	5.30

the red zone with increasing content of Tb^{3+} and almost becomes constant when the total content of Tb^{3+} and Eu^{3+} is over 30.5% and 45.5% for GdBO$_3$ and Na$_2$Gd$_2$B$_2$O$_7$, respectively. The experimental values are amazingly close to the predicted ones which are 32.31%−32.54% and 44.33%− 44.48% even though the hosts are very different. This indicates the universal applicability of the empirical saturation distance in phosphate and borate. Conversely, the saturation distance R(Tb^{3+}−Eu^{3+}) for GdBO$_3$ and Na$_2$Gd$_2$B$_2$O$_7$ can be calculated according to the chromaticity coordinate with eq 1. The calculated values are 7.09 and 6.89 Å for GdBO$_3$ and Na$_2$Gd$_2$B$_2$O$_7$, respectively, being very close to that for YPO$_4$, 6.94 Å. For Na$_2$Y$_2$B$_2$O$_7$,[19] the saturation distance is obtained as being ∼6.9 Å. All the results suggest that there is an empirical saturation distance for the terbium bridge in various inorganic hosts, and the value is within the range of 6.89−7.09 Å. The ET process is sufficient when the average distance of Tb^{3+}−Eu^{3+} is

10796

dx.doi.org/10.1021/am5027924 | ACS Appl. Mater. Interfaces 2014, 6, 10792−10801

lower than this empirical value. The f electrons are shielded so that the luminescence properties of Tb^{3+} and Eu^{3+} are not sensitive to the environment. Therefore, the empirical saturation distance is feasible in different hosts.

It is important to note that the empirical saturation distance of $Tb^{3+}-Eu^{3+}$ is applicable to situations in which the content of Eu^{3+} is low ($\leq 1\%$) because a higher content of Eu^{3+} not only enhances the ET from Tb^{3+} to Eu^{3+}, leading to a weaker Tb^{3+} emission and a constant chromaticity coordinate, but also enhances the MMCT effect between Ce^{3+} and Eu^{3+}, which seriously quenches the luminescence. Therefore, it is not feasible to dope a high concentration of Eu^{3+} ions in the terbium bridge of $Ce^{3+} \rightarrow (Tb^{3+})_n \rightarrow Eu^{3+}$. A high content of Tb^{3+} ions can shorten the distance of $Tb^{3+}-Eu^{3+}$ and increase the ET possibility from Tb^{3+} to Eu^{3+}. In addition, the ET efficiency from Ce^{3+} to Tb^{3+} increases extremely as the distance of Ce^{3+} and Tb^{3+} decreases. Then the emission of Ce^{3+} becomes unobvious, having little impact on the emitting color and chromaticity coordinate. Hence, the empirical value of saturation distance is instructive for research efforts focused on introducing $S \rightarrow (Tb^{3+})_n \rightarrow A$ in other hosts with a low concentration of activator ions (Eu^{3+}).

3.4. Mechanism of Energy Transfer from S to A in S $\rightarrow$ $(Tb^{3+})_n \rightarrow$ A. The average distance between Tb^{3+} ions was considered, and the cascade model of terbium chain ($Tb^{3+}-Tb^{3+}-Tb^{3+}-...$) was put forward to explain the ET of S to A in $S \rightarrow (Tb^{3+})_n \rightarrow A$.[16,19] Nevertheless, no direct evidence supports the long-range cascade ET of "$Tb^{3+}-Tb^{3+}-Tb^{3+}-...$" and such an ET process is unreasonable for the following reasons.

First, the ET process always takes place from the high energy sensitizer to the low energy activator.

Then, the probability of ET between $Tb^{3+}-Tb^{3+}$ is low due to the little overlap between the PLE and PL spectra of Tb^{3+}.[26,31–33]

And finally, the probability for the cascade ET goes down exponentially.

As shown in Figure 7a, with the assumption that the ET probability of $Tb^{3+}-Tb^{3+}$ is p ($p < 1$), then the probability of n-grade cascade ET, P, equals p^n, which is extremely low when the n value in $(Tb^{3+})_n$ is larger than 5. That is to say, the ET from S to A via the terbium chain ($Tb^{3+}-Tb^{3+}-Tb^{3+}-...$) is a small probability event. Therefore, the cascade model of the terbium chain is infeasible.
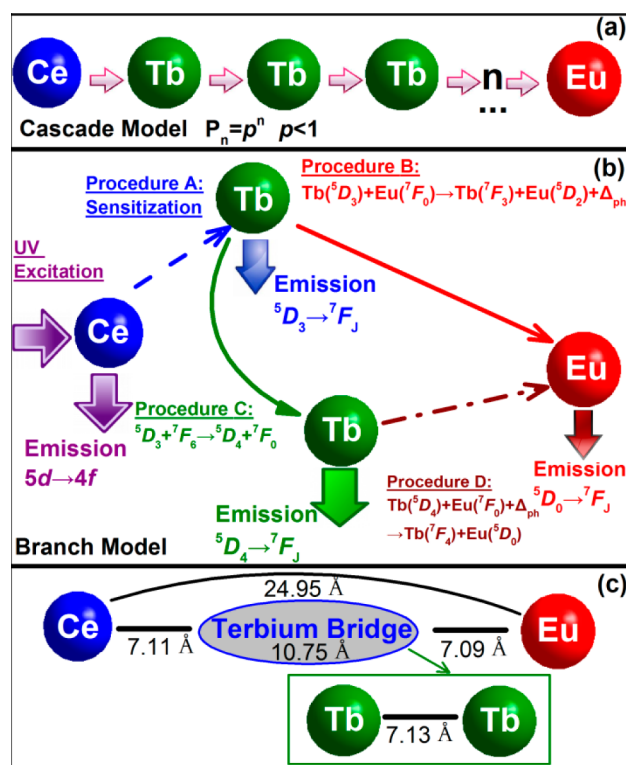
Here, we put forward the branch model to explain the whole process of ET for the terbium bridge in Figure 7b and Figure S1. The whole process consists of four procedures.

Procedure A. Ce^{3+} ions, excited by UV light, may give out an emission or sensitize Tb^{3+} ions in the ground state. The interaction between $Ce^{3+}-Tb^{3+}$ is very common and proved to be very effective by many works.[34–36]

Procedure B. The excited Tb^{3+} ions may give out a weak blue emission of $^5D_3 \rightarrow {}^7F_J$ or transfer the energy to Eu^{3+} in the way of $Tb^{3+}(^5D_3) + Eu^{3+}(^7F_0) \rightarrow Tb^{3+}(^7F_3) + Eu^{3+}(^5D_2) + \Delta_{ph}$,[37–40] where Δ_{ph} is the phonon energy.

Procedure C. Besides procedure B, an excited Tb^{3+} ion may release the energy in the way of cross-relaxation with another terbium(III) ion in the ground state: $Tb^{3+}(^5D_3) + Tb^{3+}(^7F_6) \rightarrow Tb^{3+}(^5D_4) + Tb^{3+}(^7F_0)$, which is in favor of the green emission of $^5D_4 \rightarrow {}^7F_J$.[41,42]

Procedure D. The energy of Tb^{3+} in $^5D_4$ can also flow to Eu^{3+} through the process of $Tb^{3+}(^5D_4) + Eu^{3+}(^7F_0) + \Delta_{ph} \rightarrow Tb^{3+}(^7F_4) + Eu^{3+}(^5D_0)$.[40,43]


Figure 7. Energy transfer models of terbium chain (a) and terbium bridge (b), and the distances between rare earth ions in $Ce^{3+} \rightarrow (Tb^{3+})_n \rightarrow Eu^{3+}$ (c).

The Eu^{3+} ions are sensitized by Tb^{3+} unaffected by the procedure that is followed, which is consistent with the decreasing average time of Tb^{3+} in Figure 3a, b and Table 1. Moreover, the PLE spectra of $Ba_3Lu(PO_4)_3$:$w$$Tb^{3+}$,1%$Eu^{3+}$ and $TbPO_4$:1%Eu^{3+} in Figures 2a and 4a demonstrate that the emission of Eu^{3+} originates from the $^5D_3$ (377–378 nm) and $^5D_4$ (488 nm) energy levels of Tb^{3+}, corresponding to procedures B and D. The values of distances between rare earth ions are calculated with eq 1 and presented in Table S4 to further confirm the branch model. For $GdBO_3$:0.2%Ce^{3+},30%Tb^{3+},0.5%Eu^{3+}, the average distances of Ce–Eu, Ce–Tb, and Tb–Eu are 24.95, 7.11, and 7.09 Å, respectively. Therefore, the length of the intermediary system $(Tb^{3+})_n$ is estimated to be 10.75 Å, being about 1.5 times the average distance of Tb–Tb as shown in Figure 7c. This indicates that there are two or three terbium ions between Ce^{3+} and Eu^{3+} ions in the $Ce^{3+} \rightarrow (Tb^{3+})_n \rightarrow Eu^{3+}$ system. The result is similar for $Na_2Gd_2B_2O_7$:0.2%Ce^{3+},45%Tb^{3+},0.5%Eu^{3+}. Consequently, the branch model is more appropriate than the cascade one because the ET process is completed with only two or three terbium ions.

The ET of $Ce^{3+}-Tb^{3+}$ is efficient; however, the efficiency of ET in $Tb^{3+}-Eu^{3+}$ is poor due to the extremely unobvious overlap of the PLE spectrum of Eu^{3+} and the PL of Tb^{3+}. Therefore, it is necessary to raise the content of Tb^{3+} to shorten the average distance of $Tb^{3+}-Eu^{3+}$ and increase the probability of ET in procedures B and D. Furthermore, the decay time for $5d \rightarrow 4f$ of Ce^{3+} is as short as nanoseconds, while the values for $^5D_4 \rightarrow {}^7F_J$ of Tb^{3+} and $^5D_0 \rightarrow {}^7F_J$ of Eu^{3+} are on the order of microseconds, so Tb^{3+} ions also play the role of storing the energy from Ce^{3+}.[44,45]

3.5. Sensitizer-Free Terbium Bridge in GdBO$_3$. A sensitizer-free terbium bridge like $(Tb^{3+})_n$–Eu^{3+} is ideal because the MMCT quenching effect[46] between Ce^{3+}–Eu^{3+} is totally eliminated and the content of Eu^{3+} can be increased to further enhance the ET of $Tb^{3+} \rightarrow Eu^{3+}$. However, the allowed f–d transition of the sensitizer is valuable. An intensity comparison of different forms, $(Tb^{3+})_n$–Eu^{3+} versus Ce^{3+}–$(Tb^{3+})_n$–Eu^{3+}, was performed in GdBO$_3$ ascribed to dual characters of sensitizer. The PLE spectra of GdBO$_3$:Tb^{3+},Eu^{3+} are presented in Figure 8a. The intensity of the $^7F_0 \rightarrow {}^5L_6$
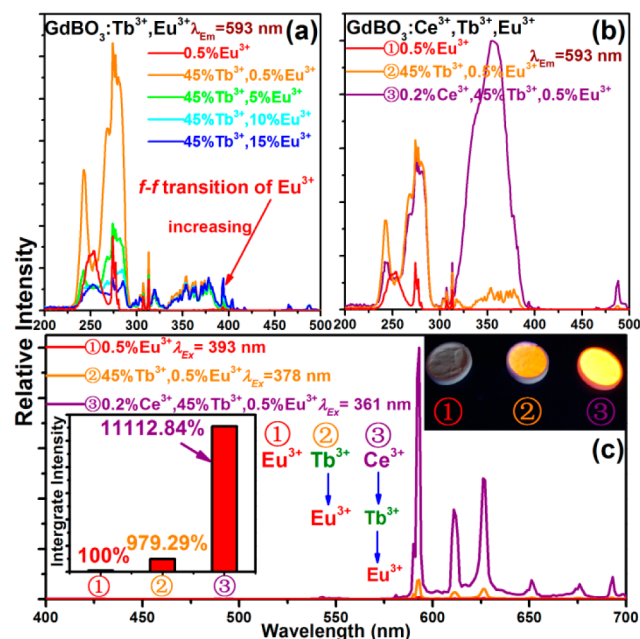

Figure 8. Photoluminescence excitation (λ_{Em} = 593 nm) and photoluminescence spectra with various doping contents of rare earth ions in GdBO$_3$:Tb^{3+},Eu^{3+} (a) and GdBO$_3$:Ce^{3+},Tb^{3+},Eu^{3+} (b), photoluminescence spectra of GdBO$_3$:Eu^{3+} with presence or absence of Ce^{3+} or Tb^{3+} (c), and comparison of the integrated intensity and photos of the corresponding samples in 365 nm UV box (inset in (c)).

transition ($\sim$393 nm) of Eu^{3+} increases slightly with increasing content of Eu^{3+}. However, the transition intensity of Tb^{3+} within the scope of 330–385 nm and the corresponding emission of the samples as shown in Figure S2 almost remain constant, indicating that the increasing concentration of Eu^{3+} has little influence on the luminescence enhancement by Tb^{3+} $\rightarrow$ Eu^{3+} excited with n-UV light. Comparison of PLE and PL spectra of GdBO$_3$:0.5%Eu^{3+}(1), GdBO$_3$:45%Tb^{3+},0.5%Eu^{3+}(2), and GdBO$_3$:0.2%Ce^{3+},45%Tb^{3+},0.5%Eu^{3+}(3) are depicted in Figure 8b and c, respectively. In Figure 8b, sample 2 produces an obvious excitation in the n-UV region compared with sample 1. Furthermore, sample 3 has a dominant excitation band attributed to the f–d transition of Ce^{3+}, which demonstrates the enhancement effect of Ce^{3+} ions for the terbium bridge in the n-UV region. As presented in Figure 8c, the emission intensity is enhanced 9.79 times with sensitization of Tb^{3+} ions and 111.12 times with sensitization of Ce^{3+} and Tb^{3+} ions, which demonstrates the more efficient sensitization effect of the Ce^{3+}–$(Tb^{3+})_n$–Eu^{3+} form compared to the $(Tb^{3+})_n$–Eu^{3+} one in the n-UV region. However, the red/orange (R/O) ratio is less than 1 due to the dominant $^5D_0$–$^7F_1$ transition. The R/O ratio may increase with increasing content of Eu^{3+} according to the theoretical research.[47] Nevertheless, the increasing content

of Eu^{3+} aggravates the MMCT effect and the emission intensity decreases. This is the dilemma to be solved in the future.

3.6. Mechanism of Luminescence Quenching of Eu^{3+} Activated by Terbium Bridge. The luminescence quenching of Eu^{3+} activated by the terbium bridge with a high content of Tb^{3+} was observed and reported in previous works.[19,20] Nevertheless, the quenching mechanism is unclear. Jia et al.[20] suggested that the concentration quenching of Tb^{3+} is the dominant mechanism, while we suggested that the ratio of Tb^{3+}/Y^{3+} has a dominant influence on the emission intensity because Tb^{3+} and Y^{3+} ions are high content components in the host matrix.[19] The critical concentration of Tb^{3+} is 10% in the Na$_2$Ln$_2$B$_2$O$_7$ (Ln = Y or Gd) system;[19,48] however, the emission quenching of Eu^{3+} is observed when the content of Tb^{3+} is over 60% for Na$_2$Y$_2$B$_2$O$_7$[19] and over 45% for Na$_2$Gd$_2$B$_2$O$_7$ as shown in Figure 9a, indicating that the concentration quenching of Tb^{3+} might be a secondary factor for decreasing the luminescent intensity of Eu^{3+}.
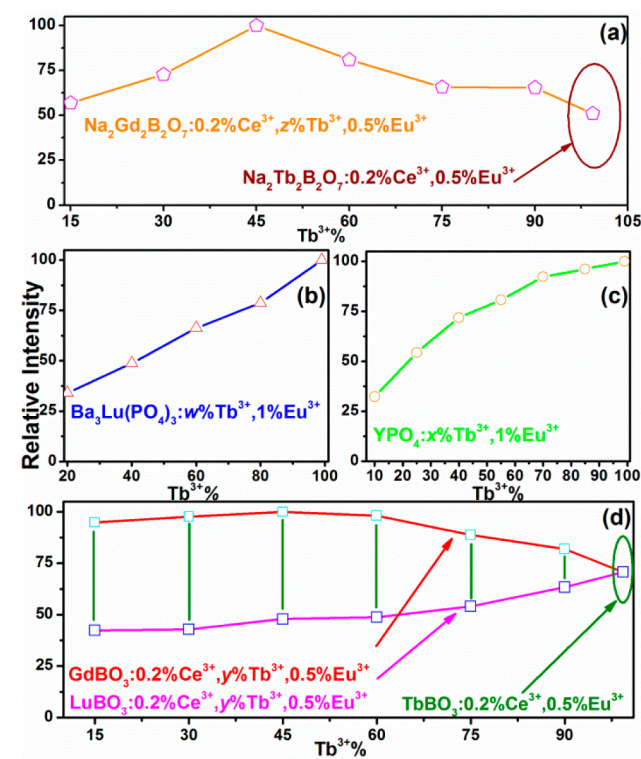
Figure 9. Integrated intensity of the emission for Na$_2$Gd$_2$B$_2$O$_7$:0.2% Ce^{3+},zTb^{3+},0.5%Eu^{3+} (a), Ba$_3$Lu(PO$_4$)$_3$:wTb^{3+},1%Eu^{3+} (b), YPO$_4$:zTb^{3+},1%Eu^{3+} (c), and LnBO$_3$:0.2%Ce^{3+},yTb^{3+},0.5%Eu^{3+} (Ln = Lu or Gd) (d).

As shown in Figure 9b–d, the changing trends of Ba$_3$Lu(PO$_4$)$_3$:wTb^{3+},1%Eu^{3+}, YPO$_4$:xTb^{3+},1%Eu^{3+}, and LuBO$_3$:0.2%Ce^{3+},yTb^{3+},0.5%Eu^{3+}, in which the emission intensity increases with the increase in concentration of Tb^{3+} to nearly 100%, further demonstrate the minor influence of concentration quenching of Tb^{3+} and the importance of the ratio of elements. Conversely, the introduction of Lu^{3+} into LnBO$_3$ quenches the luminescence of Eu^{3+}. The changing trends for GdBO$_3$ and LuBO$_3$ are different as shown in Figure 9d, though the crystal structure and the distances between Ln^{3+} ions are similar. With increasing content of Tb^{3+}, the luminescent intensity of GdBO$_3$:0.2%Ce^{3+},yTb^{3+},0.5%Eu^{3+}

increases first and then decreases when *y* is over 45%, and finally reaches the intersection point (TbBO$_3$:0.2%Ce^{3+},0.5% Eu^{3+}) with the trend line of LuBO$_3$:0.2%Ce^{3+},*y*Tb^{3+},0.5%Eu^{3+}, indicating that the variation in luminescent intensity is a result of the different ratio of elements constituting the host matrix. Similar phenomena were reported in Ca$_8$MgR-(PO$_4$)$_7$:Eu^{2+},Mn^{2+} (R = Y, La),[49] Ba$_2$Ln(BO$_3$)$_2$Cl:Eu (Ln = Y, Gd, Lu),[17] and Sr$_8$MgLn(PO$_4$)$_7$:Eu^{2+} (Ln = Y, La).[50] Terbium(III) ions, as a high content substituting element, are suggested to work as crystal constructing components to affect the luminescent intensity based on the results above. In LnBO$_3$:Ce^{3+},Tb^{3+},Eu^{3+}, a high content of Tb^{3+} may lower the emission intensity and Lu^{3+} lowers the intensity even more, once more demonstrating that concentration quenching of Tb^{3+} is the secondary cause because the concentration of Tb^{3+} decreases and the quenching effect of Tb^{3+} is weakened when Lu^{3+} is taking the place of Tb^{3+}.

Nevertheless, how the ratio of rare earth ions (Gd^{3+}/Tb^{3+}/Lu^{3+}) affects the luminescent intensity is still unknown. The radii of ions are considered. The radii of Gd^{3+}, Tb^{3+}, and Lu^{3+} are 0.938, 0.923, and 0.861 Å, respectively, with a *CN* of 6 in LnBO$_3$. When the Ln^{3+} sites are occupied successively by Gd^{3+}, Tb^{3+}, and Lu^{3+}, the radii of the ions are decreasing continuously and the luminescence is quenching as well. It is possible that the decreasing radius reduces the cell volume and the distance between the ions (Ce^{3+} and Eu^{3+}), which enhances the MMCT effect.[46] However, the consistency of the radius decreasing and luminescence quenching is no more than a coincidence. In Na$_2$Y$_2$B$_2$O$_7$:Ce^{3+},Tb^{3+},Eu^{3+}, Y^{3+} ions are replaced by Tb^{3+} with a larger radius, the emission is still quenched.[19] Therefore, there is no necessary connection between the radii-distances effect and the luminescence quenching phenomenon.

It is well-known that the surface state may impressively alter the luminescence properties of phosphors.[51] The surface defects serve as quenching centers and, thus, play important roles in the fluorescence quenching.[52−54] Therefore, the quenching effect might be a result of the increasing quantity for surface defects, which originate from the changing ratio of rare earth ions (Gd^{3+}/Tb^{3+}/Lu^{3+}).[55,56] Such defects can absorb the energy from the luminescence centers by the process of ET. Therefore, we put forward a hypothesis to explain the luminescence quenching phenomenon in the terbium bridge: the ratio of rare earth ions has an influence on the surface states of the phosphors and finally affects the quantity of surface defects and the emission intensity of Eu^{3+}. In LnBO$_3$:0.2% Ce^{3+},0.5%Eu^{3+} (Ln = Gd^{3+}, Tb^{3+}, Lu^{3+}), a higher content of Tb^{3+} creates more quenching centers, which quenches the luminescence. This quenching phenomenon is even more serious when Lu^{3+} is doped.

Luminescence decay time measurement was performed to confirm the hypothesis and the effect of quenching centers. As depicted in Figure 10, the decay time of Eu^{3+} decreases when the ratio of Tb^{3+} increases and the decreasing trend is even more obvious when Lu^{3+} ions are doped. Usually the decrease of luminescence decay time is a result of ET.[57] However, Eu^{3+} ions do not serve as sensitizers in the LnBO$_3$ system due to the absence of appropriate activators. Furthermore, the possibility of self-quenching is ruled out because the content of Eu^{3+} is as low as 0.5%. Therefore, the energy of Eu^{3+} is transferred to quenching centers (receptors) and, thus, leads to the decrease of emission intensity and decay time of Eu^{3+}. The result of the luminescence decay time measurement is well consistent with the defect-quenching hypothesis as mentioned above. We can
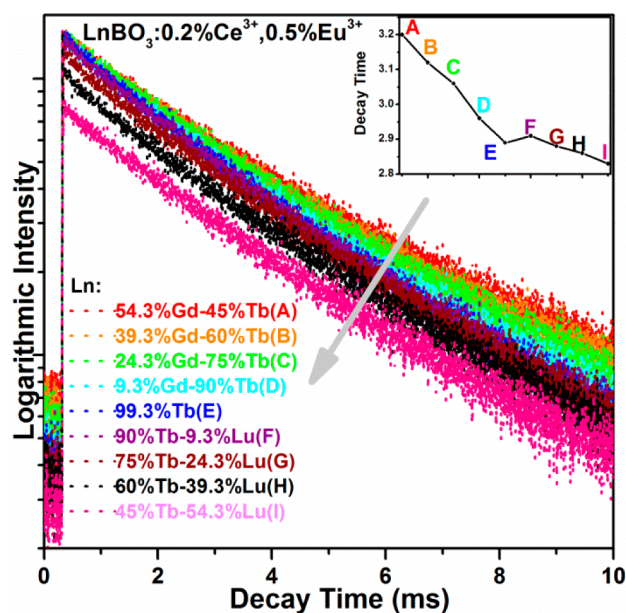
Figure 10. Luminescence decay time of Eu^{3+} in LnBO$_3$:0.2%Ce^{3+},0.5% Eu^{3+} (Ln = Gd^{3+}/Tb^{3+}/Lu^{3+}) samples and the corresponding average decay time (inset) (λ_{Ex} = 361 nm, λ_{Em} = 593 nm).

draw a conclusion that the increasing ratio of some ions may create more defects and finally generate a quenching effect in the system of the terbium bridge with the form of S−(Tb^{3+})$_n$−A. How the ratio affects the surface states is still an unsolved problem. To overcome the defect-quenching effect, it is suggested that the number of defects be decreased by the method of controlling the temperature, synthesis time, and adding flux.[58]

4. CONCLUSIONS

In summary, Ba$_3$Ln(PO$_4$)$_3$, LnPO$_4$, LnBO$_3$, and Na$_2$Ln$_2$B$_2$O$_7$ doping with various contents of Ce^{3+}, Tb^{3+}, and Eu^{3+} were synthesized. All the cell parameters were calculated with Rietveld refinement for estimating the average distances of rare earth ions. The saturation distance of Tb^{3+}−Eu^{3+} ions is estimated to be 6.89−7.09 Å in phosphates with the empirical data of hosts and is proved to be applicable to borates and other inorganic hosts with the terbium bridge. The chromaticity coordinate remains constant when the distance of Tb^{3+}−Eu^{3+} is shorter than the empirical saturation distance, or the concentration of Tb^{3+} exceeds the corresponding saturation concentration. As the distance of Tb^{3+}−Eu^{3+} is shorter than the saturation distance, the energy is almost transferred from Tb^{3+} to Eu^{3+} so that the green emission of Tb^{3+} disappears. Then the chromaticity coordinate remains constant. And the terbium bridge of S → (Tb^{3+})$_n$ → A is proved to be able to form in various inorganic hosts. The branch model for the ET of Ce^{3+}−(Tb^{3+})$_n$−Eu^{3+} is put forward to explain the role of (Tb^{3+})$_n$ in the ET from Ce^{3+} to Eu^{3+} and the necessity for a high content of Tb^{3+}. The term "terbium bridge" is used to replace "terbium chain" to show the roles of (Tb^{3+})$_n$ in the ET process of Ce^{3+}−(Tb^{3+})$_n$−Eu^{3+}, and the value of *n* is determined to be two or three. The comparison of luminescent intensity demonstrates that the S → (Tb^{3+})$_n$ → A form terbium bridge is more ideal than the sensitizer-free one even though the latter can be enhanced by increasing the content of Eu^{3+}. Finally, the mechanism for quenching the emission of Eu^{3+} with a high

content of Tb^{3+} is proposed, and the ratio of host constituting ions is thought to respond to the quantity of defects in the crystal and has a great influence on the luminescent intensity. In other words, the defect-quenching effect should be responsible for quenching the emission of Eu^{3+} activated by the terbium bridge with a high Tb^{3+} content. Based on the above-mentioned conclusions regarding the terbium bridge, we can estimate the saturation concentration of Tb^{3+} in other hosts for the terbium bridge with the value of saturation distance (~ 6.9 Å) for $Tb^{3+}-Eu^{3+}$ and optimize the luminescence properties of Eu^{3+} activated by the terbium bridge by the method of controlling the number of surface defects in the phosphors.

■ ASSOCIATED CONTENT

Ⓢ Supporting Information

Additional tables and figures. This material is available free of charge via the Internet at http://pubs.acs.org.

■ AUTHOR INFORMATION

Corresponding Authors
*E-mail: cessjx@mail.sysu.edu.cn (J.S.).
*E-mail: ceswmm@mail.sysu.edu.cn (M.W.).

Notes

The authors declare no competing financial interest.

■ REFERENCES

(1) Lin, C. C.; Liu, R.-S. Advances in Phosphors for Light-emitting Diodes. *J. Phys. Chem. Lett.* **2011**, *2*, 1268−1277.

(2) Hashimoto, T.; Wu, F.; Speck, J. S.; Nakamura, S. A GaN Bulk Crystal with Improved Structural Quality Grown by The Ammono-thermal Method. *Nat. Mater.* **2007**, *6*, 568−571.

(3) Höppe, H. A. Recent Developments in the Field of Inorganic Phosphors. *Angew. Chem., Int. Ed.* **2009**, *48*, 3572−3582.

(4) Ye, S.; Xiao, F.; Pan, Y. X.; Ma, Y. Y.; Zhang, Q. Y. Phosphors in Phosphor-Converted White Light-Emitting Diodes: Recent Advances in Materials, Techniques and Properties. *Mater. Sci. Eng., R* **2010**, *71*, 1−34.

(5) Huang, W.-Y.; Yoshimura, F.; Ueda, K.; Shimomura, Y.; Sheu, H.-S.; Chan, T.-S.; Chiang, C.-Y.; Zhou, W.; Liu, R.-S. Chemical Pressure Control for Photoluminescence of $MSiAl_2O_3N_2$:Ce^{3+}/Eu^{2+} (M = Sr, Ba) Oxynitride Phosphors. *Chem. Mater.* **2014**, *26*, 2075−2085.

(6) Dhanaraj, J.; Jagannathan, R.; Kutty, T. R. N.; Lu, C.-H. Photoluminescence Characteristics of Y_2O_3:Eu^{3+} Nanophosphors Prepared Using Sol−Gel Thermolysis. *J. Phys. Chem. B* **2001**, *105*, 11098−11105.

(7) Li, J.-G.; Li, X.; Sun, X.; Ishigaki, T. Monodispersed Colloidal Spheres for Uniform Y_2O_3:Eu^{3+} Red-Phosphor Particles and Greatly Enhanced Luminescence by Simultaneous Gd^{3+} Doping. *J. Phys. Chem. C* **2008**, *112*, 11707−11716.

(8) Guo, C.; Luan, L.; Chen, C.; Huang, D.; Su, Q. Preparation of Y_2O_2S:Eu^{3+} Phosphors by a Novel Decomposition Method. *Mater. Lett.* **2008**, *62*, 600−602.

(9) Kuang, J.; Liu, Y.; Yuan, D. Preparation and Characterization of Y_2O_2S:Eu^{3+} Phosphor via One-Step Solvothermal Process. *Electrochem. Solid-State Lett.* **2005**, *8*, H72−H74.

(10) Setlur, A. A.; Heward, W. J.; Gao, Y.; Srivastava, A. M.; Chandran, R. G.; Shankar, M. V. Crystal Chemistry and Luminescence of Ce^{3+}-Doped $Lu_2CaMg_2(Si,Ge)_3O_{12}$ and Its Use in LED Based Lighting. *Chem. Mater.* **2006**, *18*, 3314−3322.

(11) Deng, D.; Yu, H.; Li, Y.; Hua, Y.; Jia, G.; Zhao, S.; Wang, H.; Huang, L.; Li, Y.; Li, C.; Xu, S. $Ca_4(PO_4)_2O$:Eu^{2+} Red-Emitting Phosphor for Solid-State Lighting: Structure, Luminescent Properties and White Light Emitting Diode Application. *J. Mater. Chem. C* **2013**, *1*, 3194−3199.

(12) Blasse, G.; Bril, A. Study of energy transfer from Sb^{3+}, Bi^{3+}, Ce^{3+} to Sm^{3+}, Eu^{3+}, Tb^{3+}, Dy^{3+}. *J. Chem. Phys.* **1967**, *47*, 1920−1926.

(13) Bleijenberg, K. C.; Blasse, G. QMSCC Calculations on Thermal Quenching of Model Phosphor Systems. *J. Solid State Chem.* **1979**, *28*, 303−307.

(14) Blasse, G. Energy Transfer from Ce^{3+} to Eu^{3+} in $(Y, Gd)F_3$. *Phys. Status Solidi A* **1983**, *75*, K41−K43.

(15) Setlur, A. A. Sensitizing Eu^{3+} with Ce^{3+} and Tb^{3+} to Make Narrow-Line Red Phosphors for Light Emitting Diodes. *Electrochem. Solid-State Lett.* **2012**, *15*, J25−J27.

(16) Jia, Y.; Lu, W.; Guo, N.; Lu, W.; Zhao, Q.; You, H. Utilizing Tb^{3+} as an Energy Transfer Bridge to Connect $Eu^{2+}-Sm^{3+}$ Luminescent Centers: Realization of Efficient Sm^{3+} Red Emission under near-UV Excitation. *Chem. Commun.* **2013**, *49*, 2664−2666.

(17) Xia, Z.; Zhuang, J.; Meijerink, A.; Jing, X. Host Composition Dependent Tunable Multicolor Emission in the Single-Phase $Ba_2(Ln_{1-z}Tb_z)(BO_3)_2Cl$:Eu Phosphors. *Dalton Trans.* **2013**, *42*, 6327−6336.

(18) Jia, Y.; Lu, W.; Guo, N.; Lu, W.; Zhao, Q.; You, H. Realization of Color Hue Tuning via Efficient $Tb^{3+}-Mn^{2+}$ Energy Transfer in $Sr_3Tb(PO_4)_3$:Mn^{2+}, a Potential Near-UV Excited Phosphor for White LEDs. *Phys. Chem. Chem. Phys.* **2013**, *15*, 6057−6062.

(19) Wen, D.; Shi, J. A Novel Narrow-Line Red Emitting $Na_2Y_2B_2O_7$:Ce^{3+},Tb^{3+},Eu^{3+} Phosphor with High Efficiency Activated by Terbium Chain for Near-UV White LEDs. *Dalton Trans.* **2013**, *42*, 16621−16629.

(20) Jia, Y.; Lu, W.; Guo, N.; Lu, W.; Zhao, Q.; You, H. Spectral Tuning of The n-UV Convertible Oxynitride Phosphor: Orange Color Emitting Realization via an Energy Transfer Mechanism. *Phys. Chem. Chem. Phys.* **2013**, *15*, 13810−13813.

(21) Xia, Z.; Zhuang, J.; Liao, L. Novel Red-Emitting Ba_2Tb-$(BO_3)_2Cl$:Eu Phosphor with Efficient Energy Transfer for Potential Application in White Light-Emitting Diodes. *Inorg. Chem.* **2012**, *51*, 7202−7209.

(22) Barbier, J. Structural Refinements of Eulytite-Type $Ca_3Bi(PO_4)_3$ and $Ba_3La(PO_4)_3$. *J. Solid State Chem.* **1992**, *101*, 249−256.

(23) Milligan, W. O.; Mullica, D. F.; Beall, G. W.; Boatner, L. A. The Structures of Three Lanthanide Orthophosphates. *Inorg. Chim. Acta* **1983**, *70*, 133−136.

(24) Newnham, R. E.; Redman, M. J.; Santoro, R. P. Crystal Structure of Yttrium and Other Rare-Earth Borates. *J. Am. Ceram. Soc.* **1963**, *46*, 253−256.

(25) Corbel, G.; Leblanc, M.; Antic-Fidancev, E. Lemaı̈; amp; x; tre-Blaise, M., Crystal Structure of Sodium Rare Earth Oxyborates $Na_2Ln_2(BO_3)_2O$ (Ln = Sm, Eu, and Gd) and Optical Analysis of $Na_2Gd_2(BO_3)_2O$:Eu^{3+}. *J. Solid State Chem.* **1999**, *144*, 35−44.

(26) Wen, D.; Yang, H.; Yang, G.; Shi, J.; Wu, M.; Su, Q. Structure and Photoluminescence Properties of $Na_2Y_2B_2O_7$:Ce^{3+},Tb^{3+} Phosphors for Solid-State Lighting Application. *J. Solid State Chem.* **2014**, *213*, 65−71.

(27) Hoogendorp, M. F.; Schipper, W. J.; Blasse, G. Cerium(III) Luminescence and Disorder in the Eulytite Structure. *J. Alloys Compd.* **1994**, *205*, 249−251.

(28) Lai, H.; Bao, A.; Yang, Y.; Tao, Y.; Yang, H.; Zhang, Y.; Han, L. UV Luminescence Property of YPO_4:RE (RE = Ce^{3+}, Tb^{3+}). *J. Phys. Chem. C* **2007**, *112*, 282−286.

(29) Blasse, G. Energy Transfer Between Inequivalent Eu^{2+} Ions. *J. Solid State Chem.* **1986**, *62*, 207−211.

(30) Blasse, G. *Philips Res. Rep.* **1969**, *34*, P131.

(31) Duan, C.; Zhang, Z.; Rösler, S.; Rösler, S.; Delsing, A.; Zhao, J.; Hintzen, H. T. Preparation, Characterization, and Photoluminescence

Properties of Tb^{3+}-, Ce^{3+}-, and Ce^{3+}/Tb^{3+}-Activated $RE_2Si_4N_6C$ (RE = Lu, Y, and Gd) Phosphors. *Chem. Mater.* **2011**, *23*, 1851−1861.

(32) Lü, W.; Guo, N.; Jia, Y.; Zhao, Q.; Lv, W.; Jiao, M.; Shao, B.; You, H. Tunable Color of $Ce^{3+}/Tb^{3+}/Mn^{2+}$-Coactivated $CaScAlSiO_6$ via Energy Transfer: A Single-Component Red/White-Emitting Phosphor. *Inorg. Chem.* **2013**, *52*, 3007−3012.

(33) Jiao, M.; Guo, N.; Lü, W.; Jia, Y.; Lv, W.; Zhao, Q.; Shao, B.; You, H. Tunable Blue-Green-Emitting $Ba_3LaNa(PO_4)_3F:Eu^{2+},Tb^{3+}$ Phosphor with Energy Transfer for Near-UV White LEDs. *Inorg. Chem.* **2013**, *52*, 10340−10346.

(34) Xia, Z.; Liu, R.-S. Tunable Blue-Green Color Emission and Energy Transfer of $Ca_2Al_3O_6F:Ce^{3+},Tb^{3+}$ Phosphors for Near-UV White LEDs. *J. Phys. Chem. C* **2012**, *116*, 15604−15609.

(35) Geng, D.; Li, G.; Shang, M.; Yang, D.; Zhang, Y.; Cheng, Z.; Lin, J. Color Tuning via Energy Transfer in $Sr_3In(PO_4)_3:Ce^{3+}/Tb^{3+}/Mn^{2+}$ Phosphors. *J. Mater. Chem.* **2012**, *22*, 14262−14271.

(36) Kuo, T.-W.; Chen, T.-M. A Green-Emitting Phosphor $Sr_3La(PO_4)_3:Ce^{3+},Tb^{3+}$ with Efficient Energy Transfer for Fluorescent Lamp. *J. Electrochem. Soc.* **2010**, *157*, J216−J220.

(37) Yang, Z.; Huang, X.; Sun, L.; Zhou, J.; Yang, G.; Li, B.; Yu, C. Energy Transfer Enhancement in Eu^{3+} Doped $TbPO_4$ Inverse Ppal Photonic Crystals. *J. Appl. Phys.* **2009**, *105*, 083523−4.

(38) Laulicht, I.; Meirman, S. Direct Evidence for Excitation Transfer from The $^5D_4$ Manifold of Tb^{3+} to The $^5D_1$ Manifold of Eu^{3+} in $Tb_{0.66}Eu_{0.33}P_5O_{14}$. *J. Lumin.* **1986**, *34*, 287−293.

(39) Yang, J.; Zhang, C.; Li, C.; Yu, Y.; Lin, J. Energy Transfer and Tunable Luminescence Properties of Eu^{3+} in $TbBO_3$ Microspheres via a Facile Hydrothermal Process. *Inorg. Chem.* **2008**, *47*, 7262−7270.

(40) Bettinelli, M.; Speghini, A.; Piccinelli, F.; Ueda, J.; Tanabe, S. Energy Transfer Processes in $Sr_3Tb_{0.90}Eu_{0.10}(PO_4)_3$. *Opt. Mater.* **2010**, *33*, 119−122.

(41) Liu, W.-R.; Huang, C.-H.; Yeh, C.-W.; Chiu, Y.-C.; Yeh, Y.-T.; Liu, R.-S. Single-Phased White-Light-Emitting $KCaGd-(PO_4)_2:Eu^{2+},Tb^{3+},Mn^{2+}$ Phosphors for LED Applications. *RSC Adv.* **2013**, *3*, 9023−9028.

(42) Geng, D.; Shang, M.; Zhang, Y.; Lian, H.; Cheng, Z.; Lin, J. Tunable Luminescence and Energy Transfer Properties of $Ca_5(PO_4)_2SiO_4:Ce^{3+}/Tb^{3+}/Mn^{2+}$ Phosphors. *J. Mater. Chem. C* **2013**, *1*, 2345−2353.

(43) Zhang, C.; Liang, H.; Zhang, S.; Liu, C.; Hou, D.; Zhou, L.; Zhang, G.; Shi, J. Efficient Sensitization of Eu^{3+} Emission by Tb^{3+} in $Ba_3La(PO_4)_3$ under VUV−UV Excitation: Energy Transfer and Tunable Emission. *J. Phys. Chem. C* **2012**, *116*, 15932−15937.

(44) Shang, M.; Li, G.; Kang, X.; Yang, D.; Geng, D.; Lin, J. Tunable Luminescence and Energy Transfer properties of $Sr_3AlO_4F:RE^{3+}$ (RE = Tm/Tb, Eu, Ce) Phosphors. *ACS Appl. Mater. Interfaces* **2011**, *3*, 2738−2746.

(45) Zhang, L.; Zhang, J.; Zhang, X.; Hao, Z.; Zhao, H.; Luo, Y. New Yellow-Emitting Nitride Phosphor $SrAlSi_4N_7:Ce^{3+}$ and Important Role of Excessive AlN in Material Synthesis. *ACS Appl. Mater. Interfaces* **2013**, *5*, 12839−12846.

(46) Blasse, G.; Bril, A. Study of Energy Transfer from Sb^{3+}, Bi^{3+}, Ce^{3+} to Sm^{3+}, Eu^{3+}, Tb^{3+}, Dy^{3+}. *J. Chem. Phys.* **1967**, *47*, 1920−1926.

(47) Sohal, S.; Nazari, M.; Zhang, X.; Hassanzadeh, E.; Kuryatkov, V. V.; Chaudhuri, J.; Hope-Weeks, L. J.; Huang, J. Y.; Holtz, M. Effect of Tb^{3+} Concentration on The Optical and Vibrational Properties of YBO_3 Tri-Doped with Eu^{3+}, Ce^{3+}, and Tb^{3+}. *J. Appl. Phys.* **2014**, *115*, 183505.

(48) Guo, C.; Jing, H.; Li, T. Green-Emitting Phosphor $Na_2Gd_2B_2O_7:Ce^{3+}$, Tb^{3+} for Near-UV LEDs. *RSC Adv.* **2012**, *2*, 2119−2122.

(49) Wen, D.; Dong, Z.; Shi, J.; Gong, M.; Wu, M. Standard White-Emitting $Ca_8MgY(PO_4)_7:Eu^{2+},Mn^{2+}$ Phosphor for White-Light-Emitting LEDs. *ECS J. Solid State Sci. Technol.* **2013**, *2*, R178−R185.

(50) Huang, C.-H.; Chen, T.-M. Novel Yellow-Emitting $Sr_8MgLn-(PO_4)_7:Eu^{2+}$ (Ln = Y, La) Phosphors for Applications in White LEDs with Excellent Color Rendering Index. *Inorg. Chem.* **2011**, *50*, 5725−5730.

(51) Saha, S.; Das, S.; Ghorai, U. K.; Mazumder, N.; Gupta, B. K.; Chattopadhyay, K. K. Charge Compensation Assisted Enhanced Photoluminescence Derived from Li-Codoped $MgAl_2O_4:Eu^{3+}$ Nanophosphors for Solid State Lighting Applications. *Dalton Trans.* **2013**, *42*, 12965−12974.

(52) Balakrishnaiah, R.; Yi, S. S.; Jang, K.; Lee, H. S.; Moon, B. K.; Jeong, J. H. Enhanced Luminescence Properties of $YBO_3:Eu^{3+}$ Phosphors by Li-Doping. *Mater. Res. Bull.* **2011**, *46*, 621−626.

(53) Yang, H. K.; Choi, H.; Moon, B. K.; Choi, B. C.; Jeong, J. H.; Kim, J. H.; Kim, K. H. Improved Luminescent Behavior of $YVO_4:Eu^{3+}$ Ceramic Phosphors by Li Contents. *Solid State Sci.* **2010**, *12*, 1445−1448.

(54) Mu, Z.; Hu, Y.; Chen, L.; Wang, X. Enhanced Red Emission in $ZnB_2O_4:Eu^{3+}$ by Charge Compensation. *Opt. Mater.* **2011**, *34*, 89−94.

(55) Szczeszak, A.; Grzyb, T.; Barszcz, B.; Nagirnyi, V.; Kotlov, A.; Lis, S. Hydrothermal Synthesis and Structural and Spectroscopic Properties of the New Triclinic Form of $GdBO_3:Eu^{3+}$ Nanocrystals. *Inorg. Chem.* **2013**, *52*, 4934−4940.

(56) Lorbeer, C.; Mudring, A.-V. White-Light-Emitting Single Phosphors via Triply Doped LaF_3 Nanoparticles. *J. Phys. Chem. C* **2013**, *117*, 12229−12238.

(57) Dobrowolska, A.; Zych, E. Spectroscopic Characterization of $Ca_3Y_2Si_3O_{12}:Eu^{2+},Eu^{3+}$ Powders in VUV−UV−vis Region. *J. Phys. Chem. C* **2012**, *116*, 25493−25503.

(58) Jiao, M.; Jia, Y.; Lu, W.; Lv, W.; Zhao, Q.; Shao, B.; You, H. A Single-Phase White-Emitting $Ca_2SrAl_2O_6:Ce^{3+},Li^+,Mn^{2+}$ Phosphor with Energy Transfer for UV-Excited WLEDs. *Dalton Trans.* **2014**, *43*, 3202−3209.